PROCEEDINGS, Thirty-Sixth Workshop on Geothermal Reservoir Engineering
Stanford University, Stanford, California, January 30 - February 1, 2012

# SOIL GAS FLUX EXPLORATION AT THE ROTOKAWA GEOTHERMAL FIELD AND WHITE ISLAND, NEW ZEALAND

Simon BLOOMBERG[1], Clinton RISSMANN[2], Agnes MAZOT[3], Christopher OZE[1], Travis HORTON[1], Darren GRAVLEY[1], Ben KENNEDY[1], Cynthia WERNER[4], Bruce CHRISTENSON[3] and Joanna PAWSON[1]

[1]University of Canterbury, Pvt Bag 4800, NZ
[2]Environment Southland, Pvt Bag 90116, NZ
[3]GNS Science, Pvt Bag 2000, NZ
[4]Cascades Volcano Observatory, Vancouver, Wa
E-mail: Simon.Bloomberg@pg.canterbury.ac.nz

## ABSTRACT

A significant challenge to geothermal exploration is accurate quantification of the heat and mass flow between deep reservoir(s) and the surface. Here, we use high resolution measurement of carbon dioxide ($CO_2$) flux and heat flow at the land surface to characterise the mass ($CO_2$ and steam) and heat released from the geothermal reservoir. Statistical characterisation of background soil respired $CO_2$ flux reduces the level of uncertainty when deriving mass (emissions) and heat flow estimates from high temperature reservoirs.

We report the preliminary results of two soil gas and heat flow surveys for an active andesitic stratovolcano (White Island) and a high temperature geothermal field (Rotokawa), both of which occur within the Taupo Volcanic Zone, New Zealand. The flux and heat flow surveys include over 3000 direct measurements of $CO_2$ flux, soil temperature and current and historic fumarolic discharge samples.
Initial results include a total $CO_2$ emission rate of 633 ± 16$td^{-1}$ (2.5$km^2$) for Rotokawa while at White Island we report a total $CO_2$ emission rate of 116 ± 2$td^{-1}$ for the crater floor (.3$km^2$). Using $CO_2$:$H_2O$ molar ratios the thermal energy release associated with diffuse degassing is 317MW and 54MW respectively.

These preliminary results shed light on the heat and mass flow dynamics of an active andesite volcano (White Island) and a high temperature magma-hydrothermal field (Rotokawa).

## INTRODUCTION

Heat and mass energy transfer through volcanic and hydrothermal systems in the Taupo Volcanic Zone (TVZ) of New Zealand has historically been measured using surface geophysical, geochemical and geological techniques. Modern techniques for surface measurement of heat and mass flow have advanced considerably over the last 50 years since some of the first measurements of heat and mass flow from volcanic hydrothermal systems. In particular the measurement of $CO_2$ flux and its use as a proxy for heat and mass transfer has greatly improved our understanding of the heat and mass release from high temperature reservoirs as well as the nature of structural controls over fluid flow (Chiodini et al. 2005; Fridriksson et al. 2006; Viveiros et al. 2010; Werner & Cardellini, 2006).

Numerous soil $CO_2$ flux surveys of volcanic and magma-hydrothermal systems have been undertaken over the last 20 years. Initially, flux surveys sought to better quantify the contribution of diffuse emissions from volcanic systems to the global carbon cycle. From this initial work the value of flux surveys as a method for assessing heat and mass flow and for investigating structural controls to fluid flow was recognised. Increasingly $CO_2$ flux surveys are being used by researchers of volcanic and volcanic-hydrothermal systems as well as by geothermal exploration geologists (Brombach et al., 2001; Cardellini et al., 2003; Chiodini et al., 1998; Dereindra & Armannsson, 2010; Evans et al. 2001; Mörner & Etiope, 2002; Lewicki et al., 2005; Rissmann et al., 2012).

Here we present the preliminary results of detailed $CO_2$ flux and heat flow surveys for White Island (WI), an active andesitic stratovolcano, and Rotokawa (RK) a high temperature magma-hydrothermal field, both within the TVZ of New Zealand. Total heat flow (MW) and emission rates ($td^{-1}$) are quantified for each survey along with detailed maps of the spatial extent and magnitude of soil gas flux and heat flow. Normalised total emission rates are contrasted with values reported for fields within the TVZ and internationally (Mörner and Etiope, 2002; Rissmann, 2010; Werner and Cardellini, 2006) and spatial maps of surface flux and heat flow are used to infer structural controls to fluid

flow. A comparison is also made between the observed and $CO_2$-derived heat flow estimates for both fields. Finally, the source of $CO_2$ at each field is assessed on the basis of cumulative probability plots and by comparison with $CO_2$ flux and soil temperature.

## GEOLOGICAL SETTING

### White Island

White Island (Whakaari) is an active andesitic stratovolcano located 50 km to the north east of Whakatane, on strike with the eastern edge of the TVZ. The volcano is one of New Zealand's most active volcanoes with frequent eruptions over the last 40 years (Houghton and Nairn, 1989) and numerous eruptions in historic times (Cole and Nairn, 1975; Wardell et al., 2001), the latest eruptive sequence being phreatomagmatic. The island, though being surrounded by seawater on all sides, has a semi-sealed acidic hydrothermal system (Houghton and Nairn, 1989). The gas chemistry is typical of active arc volcanism with a high gas input from subducting marine sediments (Giggenbach, 1995).

The lithology of the crater floor is comprised of volcanic sediments and ash from eruptions, landslides and ancestral crater lakes. The island is devoid of vascular plant species with the exception of the seaward flanks of the volcano. Thermal activity consists of steaming vents, active fumaroles (>220°C), acid streams and pools, steaming and boiling mud pots and pools, inactive and fossil features are numerous. The western crater is filled with a large boiling acid lake (pH ≈ -0.2) which is the centre of modern day phreatomagmatic activity. Subsurface permeability at WI is controlled by hydrothermally-altered clay cap layers within which ascending steam condenses and sulphur minerals precipitate. Areas of high permeability create degassing structures and are often linked with landslide hummocks that have infilled the crater floor during historic eruptions. Fumarolic activity has been monitored for the last 50 years (Giggenbach 1975a, 1983; Rose et al. 1996).

### Rotokawa

The geothermal system at RK has been under scientific inspection for the best part of 60 years (Hedenquist et al., 1988; references therein). The principal thermal feature is a warm (~24°C) acid (pH ≈2.2) lake with an area of ~0.62 $km^2$. Directly to the north lies an area of steaming ground, hot pools, sink holes, sulphur banks, explosion craters and fumaroles. This area has been extensively modified by surface sulphur mining activity in the past 40 years.

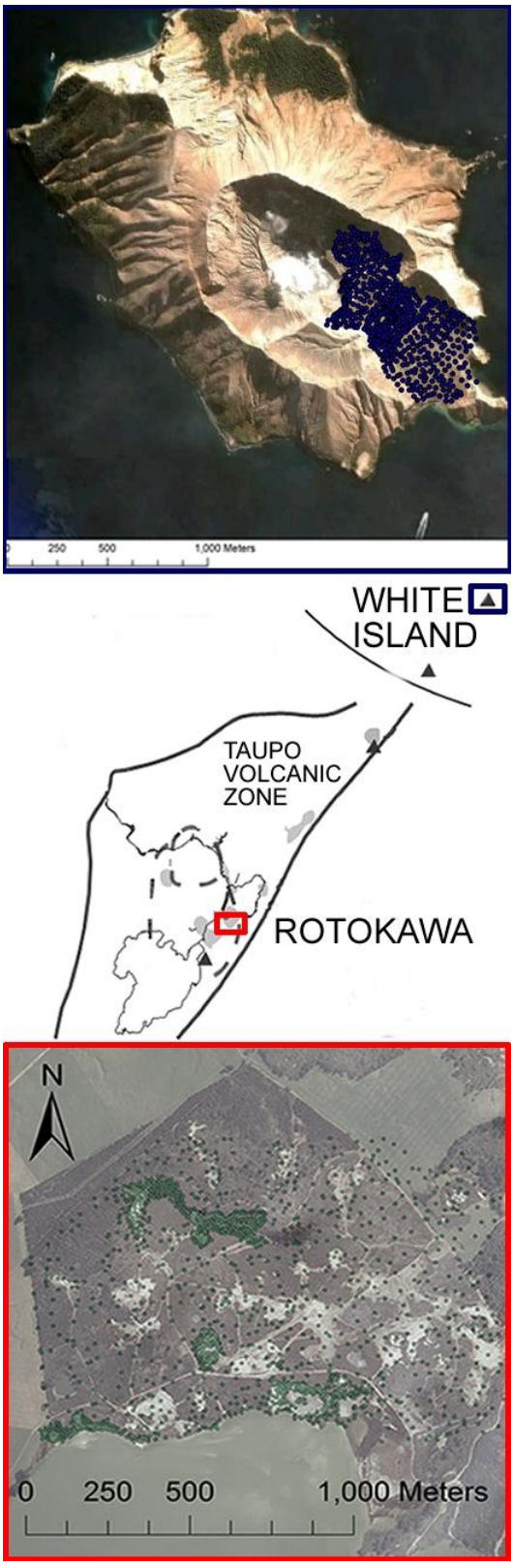

*Figure 1: Mapped locations of soil gas measurements at RK (bottom) and WI (top) with respect to the Taupo Volcanic Zone, New Zealand.*

Two geothermal power stations generate from the geothermal reservoir, Rotokawa A (34MW) and Nga Awa Purua (140 MW). The maximum fluid temperature is ~320°C, recorded within the Rotokawa andesite deep reservoir rock. Two-phase fluid flows from the deep reservoir through to the surface as the local confining cap layer (the Huka Falls Formation, a volcaniclastic lake deposit rich in clays) has been removed in this area by either hydrothermal eruptions or dissolution.

## METHODS & MATERIALS

### Field methods

Two gas measurement methods are used; soil flux surveys and subsoil gas sampling for compositional analysis of fumarolic gases (Rissmann et al., 2012).

#### *Soil gas flux ($CO_2$ and $H_2S$) and temperature measurement:*

Soil gases flux ($CO_2$ and $H_2S$) and soil temperatures were measured in the thermal areas at RK and at locations within the WI crater floor. The accumulation chamber method for measurement of soil $CO_2$ flux (lewicki et al., 2005; Chiodini et al., 2008; Rissmann et al., 2012) was used. Due to the effects of rainfall on soil gas, data was collected up to 4 days after heavy rain and 2 days after light rain (Lewicki et al. 2005). Due to the poor response of the chemical sensor very few $H_2S$ flux values were measured (~ 100). When in the field, the minor purge time between each consecutive measurement site (< 2 min) did not enable the $H_2S$ sensor to recover. Therefore, in the following paper all references to 'flux' relate to $CO_2$ unless otherwise stated.

Soil gas flux was measured using a West Systems accumulation chamber and LICOR LI-820 infrared gas analyser for $CO_2$ (after Welles et al., 2001). A mean measurement error of ±2% was assumed for $CO_2$ Flux as is discussed by Giammanco et al. (2007). Soil Temperatures were measured to 10cm depth within ~0.1m of the accumulation chamber footprint using a Yokogawa TX-10 digital thermometer and a K-type thermocouple (measurement accuracy ±0.5°c). Coordinates for each site were logged using a Garmin 60x GPS.

The flux survey design at RK used a systematic sampling approach (spacing 10 m - 20 m, depending on flux cues such as ground alteration and odour) coupled with an adaptive sampling component (Boomer et al. 2000). Adaptive sampling was initiated when a measurement exceeded the background flux level (>3ppm $s^{-1}$, ≥ambient T°C) at which point the resolution increased to 5 m spacing. Due to time constraints at WI, measurements were based on the systematic sampling approach only (Figure 1).

### Data Analysis Methods

#### *Data Analysis*

Upon entry into spreadsheet the raw (field) $CO_2$ and $H_2S$ data are converted from ppm $s^{-1}$ to g $m^{-2}$ $d^{-1}$ using an equation that takes into account the ambient temperature and atmospheric pressure. The raw soil temp values were converted from °c to W (watts) $m^{-2}$ (using formulas below). As diffuse $CO_2$ flux from soil can come from multiple sources (organic/atmospheric/magmatic) we use Sinclair's (1974) method of plotting geochemical data on a log-normal probability plot with a Gaussian distribution (cumulative probability), the dataset was broken into populations and the applied method described in Chiodini (1998) was used to find the end member and mixing populations within this studies datasets. From this graphical statistical analysis (GSA), gas-source populations were calculated. 5 populations were found for each dataset (Appendix: 1). Interpolation of un-sampled areas were modelled using the sequential Gaussian simulation (sGs) algorithm within the WinGsLib software toolbox (Deustsch & Journel, 1998), following the methods of Cardellini et al. (2003). Each simulation ran for 500 realisation at 5m cell size using variogram models (Appendix: 2) based on the direct measurements.

Total emission estimates from GSA were compared to those from sGs and the results show that GSA overestimates the contribution of hydrothermal $CO_2$ to the total flux, as is consistent with other studies (Cardellini et al., 2003; Rissmann et al., 2012) so therefore only sGs estimates for $CO_2$ emissions were used, however the cumulative probability plots were helpful in delineating the background populations in lieu of isotopic data.

#### *Heat and mass flow through soil (from soil temperature)*

Over 3000 soil temperature measurements were taken at RK and WI to a maximum depth of 15cm though most were taken at 10cm, this means when using the following formulas all deliverables will be underestimates. If the boiling point temperature (98.7

at RK and 100 at WI) was reached before 10cm this was noted. Eqs. 1 & 2. were then applied to the data based on Dawson (1964) and calibrated at the Wairakei geothermal field near Taupo. It was expected that similar conditions exist at RK and WI and therefore they can be applied without change.

Where $t_{15}$ (soil temperature at 15cm depth) is <98.7°C the soil heat flux ($q_s$ in $Wm^{-2}$) is estimated by:

Eq. 1. $q_s = 5.2 \times 10^{-6} t_{15}^4$

Where $t_{15}$ is ≥98.7°C Dawson's (1964) second equation allows estimation using the depth to 98.7°C as $d_{98.7}$ in:

Eq. 2. $q_s = 10^{\left(\frac{(Log\, d_{98.7} - 3.548)}{-0.84}\right)}$

Heat flow was then simulated using the sGs method and the observed and simulated values were compared. The individual point values are summed to determine the total heat flow through soil from the study area.

Mass flow of steam through soil ($F_{S,H_2O}$ in kg $s^{-1}$) for the study area can also be calculated using the heat flow through soil ($H_s$) and the heat in steam mass ($h_{s,100°C} - h_{w,t_r}$ ):

Eq. 3. $F_{S\,(H_2O)} = \frac{H_s}{(h_{s,100°C} - h_{w,t_r})}$

Where $H_s$ is the calculated heat flow in Watts from eq.1-2 normalised for the thermal area, $h_{s,100°C}$ is the enthalpy of steam at 100°C (2676 kJ/kg) and $h_{w,t_r}$ is the enthalpy of water at the mean annual temperature for the field areas (RK=23°C;96kJ/kg,WI=10°C:41.9kJ/kg; NIWA.co.nz 2011; Schmidt and Grigull 1979).

***Heat, mass flow and emissions calculations from $CO_2$ flux***

In order to compare the contribution of soil gas flux to total $CO_2$ emissions (in addition to boiling hot pools and fumaroles) the total volume of diffuse soil gas flux simulated measurements are summed and normalised to the area of thermal activity. In absence of a "plume" (e.g. Crater Lake at WI), the minimum contribution to total $CO_2$ emission from diffuse soil gas flux was 85% and the maximum, 100% (Dereinda & Armannsson, 2010; Fridriksson et al. 2006). At RK there are steam heated pools, active steaming vents and sulphur banks so it appears likely that the contribution of soil gas flux to the total emission value is less than 100%. At WI, which has a "plume" the contribution of soil gas to total emission rates previously were 1% (Wardell et al. 2001) and was recalculated in this study.

To calculate equivalent steam flow the molar ratio of the vapour phase is applied to the soil gas flux data using:

Eq. 4. $F_{stm(CO_2)} = F_{CO_2} \cdot \frac{[H_2O]}{[CO_2]}$

Where $F_{CO_2}$ is the total flux of $CO_2$ in g $s^{-1}$, $\frac{[H_2O]}{[CO_2]}$ is the molar ratio in g, and Fstm($CO_2$) is the steam mass flow in g $s^{-1}$. In this way we can calculate the quantity of steam mass flow that is condensed within the subsurface by comparing Fstm($CO_2$) with the value from heat flow through soil ($F_{s\,(H_2O)}$, Eq. 3).

An equivalent heat flow can be calculated for the steam mass flow (Fstm($CO_2$)) derived from Eq. 4. using the following equation:

Eq. 5. $Hs = F_{stm(CO_2)} \cdot h_{s,100°C}$

Where Fstm($CO_2$) is from Eq. 4., and is the steam flux in g $s^{-1}$, and $h_{s,100°c}$ is the enthalpy of steam at 100°C (2676 kJ/kg) and *Hs* is the heat flow in Watts.

## RESULTS

### Diffuse soil gas fluxes and soil temperatures

***Rotokawa***

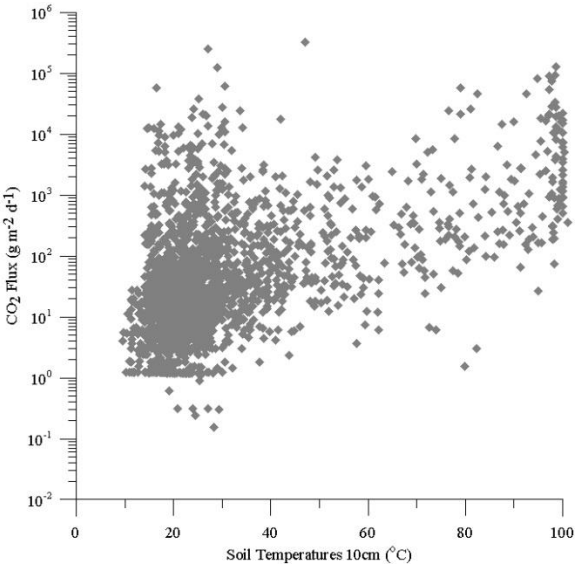


*Figure 2: Bi-modal Distribution of $CO_2$ flux and soil temperature measurements at RK.*

Diffuse soil $CO_2$ fluxes range from <0 to 322,100g $m^{-2}$ $d^{-1}$ from 2,545 direct measurements. Soil temperatures range from 9 to 100 °C. Figure 2 shows the correlation between $CO_2$ and soil temperature to be a general one with two modes of high flux with low temperatures and the other with high temperatures.

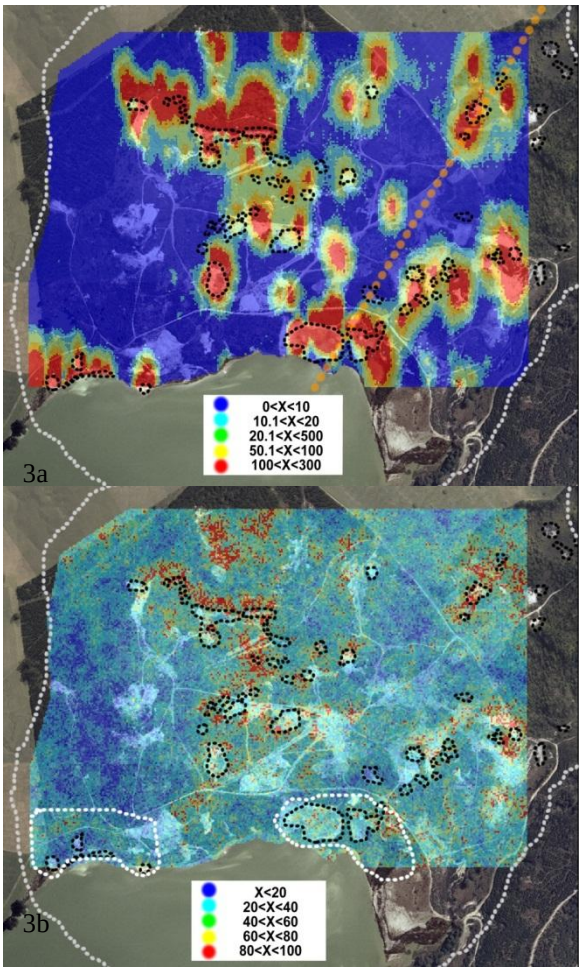


*Figure 3a: Soil $CO_2$ flux mapped within the thermal area's resistivity boundary (Hedenquist et al. 1988), the Central Field Fault (CFF) is the orange dotted line. Figure 3b: Soil Temperatures at 10cm (°C) are mapped within the thermal areas resistivity boundary and $CO_2$ anomalies with high flux but low temperatures are outlined in white. Surface thermal features are mapped with black dotted lines in each image.*

Figure 3a shows the high flux (>300 g $m^{-2}$ $d^{-1}$) anomalies are quasi-circular in nature but become more diffuse and broadly distributed at lower flux rates. There is a concentration of areas close to the lake shore as well as along an E-W trending sub-linear feature north of the lake. The highest flux values occur along the lake shore and coincide with lower average soil temperatures (<50°C) indicating some decoupling of steam flow likely due to high water tables adjacent to the lake (Figure 3b). To the north and northwest greater coupling between heat flow (high soil temperatures) and $CO_2$ flux indicates less scrubbing of the steam phase. The active thermal area has been mapped previously using resistivity boundaries and the flux map doesn't produce any anomalous flux outside of this mapped boundary.

The arithmetic declustered mean of $CO_2$ gas flux was 274 g $m^{-2}$ $d^{-1}$ while the sGs produced a mean of 246 g $m^{-2}$ $d^{-1}$. The sGs total emission rate of 340 ± 4 $td^{-1}$ was simulated in the modelled area (Figure 3a, 1.4 $km^2$). The thermal area at RK is actually larger than this, so the full thermal field minimum emissions estimate is provided by normalising the emission rate by 1.4 $km^2$ (i.e., $8.03x10^4$ t $yr^{-1}$ $km^2$) and extrapolating to 2.5 $km^2$. Extrapolation provides an emission rate of 633 ± 16$td^{-1}$ or ~50% larger. This normalised emission rate is purely for soil zone CO2 and does not include measurement of gaseous efflux from any other fluxing thermal features at RK (fumaroles, hot pools, mud pools). Removing the background contribution to the total $CO_2$ emission produces a value of 611$td^{-1}$ for hydrothermal-$CO_2$ only.

***White Island***

691 measurements of diffuse degassing were taken at WI with a range of 0.1 – 29896 g $m^{-2}$ $d^{-1}$ $CO_2$ and with soil temperatures (10 cm) of 15 to 100°C. Figure 4 shows the relationship between $CO_2$ and soil temperature at WI.

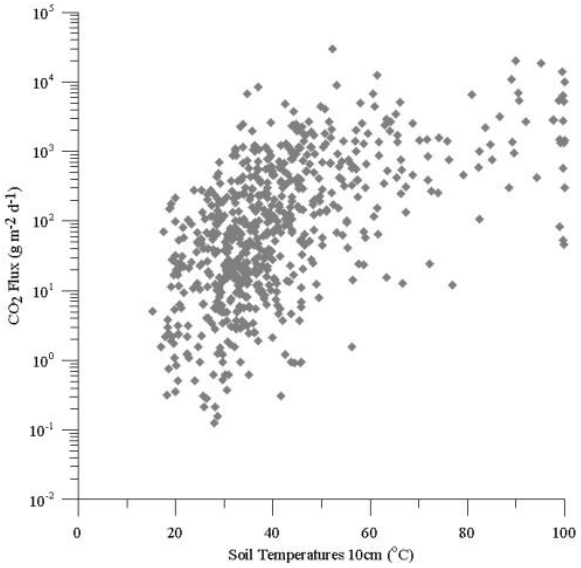


*Figure 4: The distribution of soil $CO_2$ flux and temperature (~10cm, °C) at WI. A broad positive trend is observed though there is some weak*

*separation of high $CO_2$ flux into low and high temperature modes.*

The sGs models for $CO_2$ flux (Figure 5a) show values generally diminishing from the Crater Lake to the south eastern edge of the crater floor. The most significant fluxes are centrally located in the crater near hot mud pools, sulphurous mounds and steaming ground, with the flux anomalies being concentrated and constrained to the areas surrounding these features.

Soil temperatures (Figure 5b) are in good agreement with the mapped surface features and $CO_2$ flux anomalies; there are only three areas in the crater floor which show both low temperatures and $CO_2$ Flux (Figure 5b). The arithmetic mean for declustered $CO_2$ Flux was 367 g $m^{-2}$ $d^{-1}$ which was the same as the sGs mean. From the sGs Model an emission rate of 116 ± 2$td^{-1}$ is computed for the survey area (0.31 $km^2$) within the crater floor.

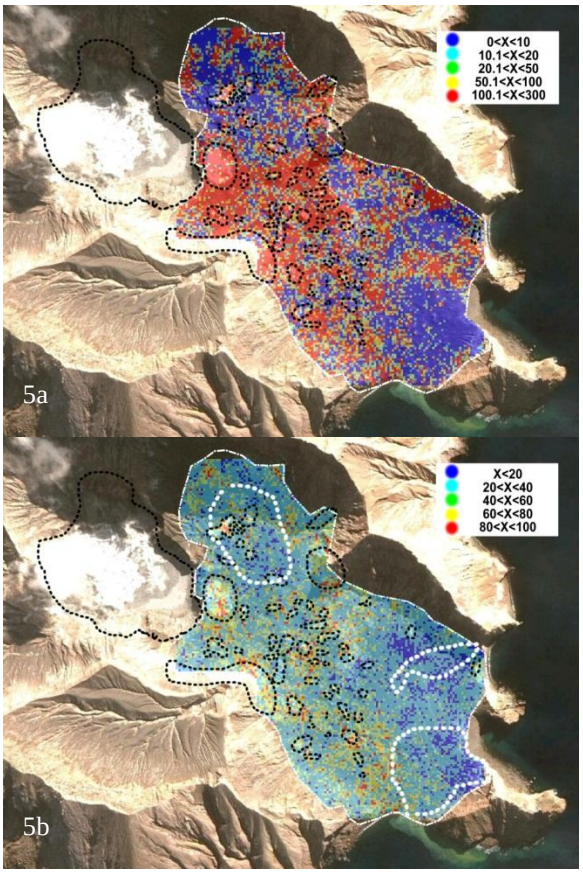


*Figure 5a: Soil $CO_2$ Flux is mapped within the accessible crater floor; surface thermal features are mapped in both figures with black dotted lines. Figure 5b: Soil temperatures at 10cm (°C) are mapped within the crater floor; areas of low temperatures & $CO_2$ flux are outlined in white.*

There are obvious flank and crater wall emissions at WI, so for the total island soil diffuse emission an area of 1.5$km^2$ is multiplied by the normalised rate (1.34x$10^5$ $tyr^{-1}km^{-2}$) and gives 576 ± 8$td^{-1}$ $CO_2$, this is a maximum total emission. Removing the background contribution to the total emission gives a value of 115$td^{-1}$for hydrothermal emissions.

***$H_2S$ Flux and relationships with CO2 at Rotokawa***

$H_2S$ flux values from 121 sites range from 0.2 to 156 g $m^{-2}$ $d^{-1}$. There is a varied spread in the data with no correlation to soil temperature due to the limited data. No $H_2S$ flux was ever measured without being in close proximity to a surface thermal feature. Out of the 121 sites only 46 have significant $H_2S$ flux (>5 g $m^{-2}d^{-1}$), while 75 of the same sites had significant $CO_2$ flux (>100 g $m^{-2}d^{-1}$). In Figure 7 we plot the fluxes comparatively and find a threshold relationship. Here $H_2S$ flux is minimal until $CO_2$ flux values exceed a threshold of ~100 g $m^{-2}d^{-1}$ at which point $H_2S$ is detected and strong correlation between both gaseous species is evident.

Two fumarole samples were used to calculate the $CO_2$:$H_2S$ ratio of surface advective steam flow (pipe flow). The range of their ratios is plotted in Figure 7. This provides an estimate of the distribution of the gas composition for advective degassing. While a few of the soil gas samples fall within this range most of the data show a higher $CO_2$:$H_2S$ ratio.

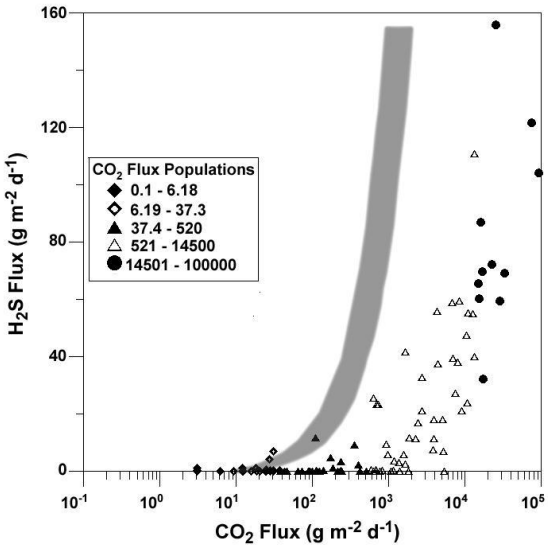


*Figure 7: Distribution of the acid soil gases at RK. Data are grouped by $CO_2$ GSA populations. The solid grey bar is the estimated fluxes based on fumarolic gas ratios.*

The $CO_2$:$H_2S$ ratio for the fumaroles has a mean of 7.9 while the mean ratio for significant soil gas flux

is 241, historic gas data from wells puts the ratio around 45 (Hedenquist et al. 1988). The trend towards a high $CO_2$:$H_2S$ ratio indicates a large portion of $H_2S$ is either scrubbed by shallow groundwater and/or precipitates as elemental S before reaching the surface of the field.

In order to produce a sulphur budget, the $CO_2$ emissions associated with all fluxes in excess of 100 g $m^{-2}$ $d^{-1}$ are multiplied by the molar $CO_2$:$H_2S$ ratio for the soil zone to produce a total $H_2S$ emission from diffuse soil degassing of 2.6 $td^{-1}$. A previous study from Lake Rotokawa found 10.38 $td^{-1}$ $SO_4^{2-}$, which equates to 3.67 $td^{-1}$ $H_2S$ (multiplying by the molar weight ratio, sulphur oxidation) (Hedenquist et al., 1988; Werner et al., 2008). This gives a minimum total surface sulphur emission for RK of 6$td^{-1}$ with a minimum total emission of $H_2S$ from the reservoir at 80$td^{-1}$ (multiplying the total $CO_2$ by the $CO_2$:$H_2S$ fumarole ratio). The loss of ~74 t d-1 of $H_2S$ within the subsurface is consistent with the extensive elemental S deposits that characterise the RK field.

## Heat flow through soil

Over 2,500 and 691 soil temperature measurements from RK and WI, respectively, were taken at depths between 0 and 10cm. Using equations 1 and 2 these were modelled with sGs then converted to heat flow in $Wm^{-2}$ and finally into a total megawatt (MW) value. For RK heat flow measurements ranged between 0.03 – 16742 with a mean of 28 $Wm^{-2}$. At WI this ranged from 0.28 – 16742 with a mean of 86.6 $Wm^{-2}$. The total heat flow through soil is estimated to be 73 ± 2.5 and 27 ± 1MW at RK and WI respectively.

### *Steam mass flow through soil*

The total heat flow through soil in watts can be used with Eq.3 to find the equivalent steam mass flow (*Fs $(H_2O)$*). At RK and WI the surface heat flow values are equivalent to 2455 $td^{-1}$ and 898 $td^{-1}$ respectively.

## Mass and heat flow from $CO_2$ degassing

Using Eqs. 4 & 5, an equivalent steam mass flow value is calculated from the $CO_2$ flux and molar $CO_2$: $H_2O$ ratio for RK and WI fumaroles.

### *Rotokawa*

In order to calculate the total heat input to RK, the total hydrothermal (611$td^{-1}$) $CO_2$ flux is multiplied by the molar ratio ($CO_2$:$H_2O$) of deep fluid, 61g$CO_2$/kg$H_2O$ or 16.6 (Hedenquist et al. 1988), to give an $F_{stm(CO_2)}$ of 10150 ± 250$td^{-1}$. From this figure a heat flow of 314 ± 7MW is calculated. The 10150$td^{-1}$ of estimated steam mass flow is equivalent to 117 ± 3$kgs^{-1}$ which is in good agreement with previous numerical model estimates for RK of 105$kgs^{-1}$ (Bowyer & Holt, 2010).

### *White Island*

The total hydrothermal-$CO_2$ emission of 115$td^{-1}$ is multiplied by the molar ratio, 65g$CO_2$/kg$H_2O$ or 15.3 (Giggenbach & Matsuo 1988), to give a steam mass flow ($F_{stm(CO_2)}$) of 1760 ± 25$td^{-1}$, from which a heat flow total of 54 ± 1MW is calculated.

## DISCUSSION

## Diffuse degassing

### *Rotokawa*

Soil gas flux measurements at RK geothermal field cover a wide range of fluxes and indicate the presence of a large gas anomaly within the thermal ground area. The mean for the total $CO_2$ population when compared with the background removed total (246 vs. 1082 g $m^{-2}$ $d^{-1}$) indicates that background fluxes must be common spatially and when removed the mean increases significantly(Figure 3a).

The total $CO_2$ emissions at RK calculated from the sGs and GSA methods have produced the greatest normalised (t $yr^{-1}$ $km^{-2}$) value in New Zealand for non volcanic emissions, at 4 times Ohaaki (Rissmann et al., 2012) and 7 times Rotorua (Werner and Cardellini, 2006). It does however compare to only half the soil gas emissions of WI (Figure 8). This indicates that though RK may not be a high gas reservoir, all of the gas that is in the system is likely to end up degassing through the thermal area.

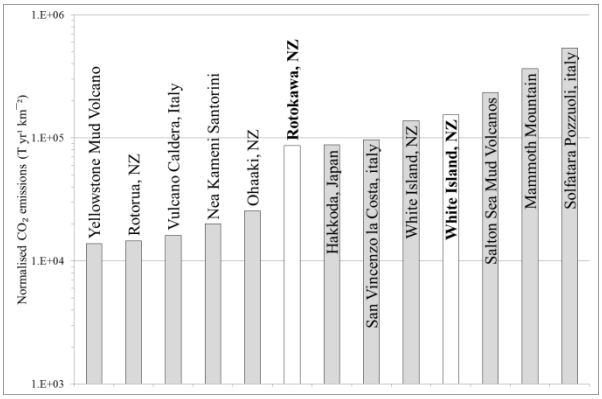


*Figure 8: Plot of thermal ground normalised CO2 emissions for this study in white and other examples in grey. (Morner and Etiope, 2002; Rissmann 2011)*

***White Island***

The difference between the total and background-removed (hydrothermal) total mean (368 vs. 723 g $m^{-2}$ $d^{-1}$) indicates a significant area has background emission which is consistent with the flux map (figures 5a). The range of flux values at WI, though not as broad as at RK does have a higher mean value, which is an indicator of the reduced contribution of background sources to the total gas emissions through the crater floor (4% background at RK vs. 1.3% background WI).

**Heat flow variables**

For both RK and WI measured soil temperature data was converted to equivalent heat flow using Eqs. 1&2, whereas heat flow based on $CO_2$ emissions was calculated using Eqs. 4&5. Both fields display lower observed heat flow than that estimated from $CO_2$ emissions. The discrepancies in heat flow values likely reflect the condensation of 77% ($241td^{-1}$) and 50% ($27td^{-1}$) of the steam phase within shallow meteoric groundwater that overlies the high temperature reservoirs at RK and WI, respectively.

Fridriksson et al. (2006) report the condensation of 87% of steam mass flow for the Reykjanes thermal area as based on the discrepancy between observed heat flow and heat flow estimated from $CO_2$ flux, which matches closely with the discrepancy at RK. White Island's hydrothermal source is shallower (~2km depth) than RK (~4km depth) and more active so there may be less steam condensate flowing out of the system. It is also notable that RK is an open system at depth and cool inflows may condense rising hydrothermal fluid. White Island has a sealed hydrothermal system (Houghton & Nairn 1989) which might encourage more steam mass flow to reach the surface in the crater area.

Historic heat flow studies at RK presented in Hedenquist et al. (1988) put the thermal energy release between 218 and 610MW, with their study finding 236MW. These studies are all based on chloride measurements which can be less robust than $CO_2$ and less mobile than the gas phase. For groundwater having reached saturation with respects to $CO_2$, the majority of the gas passes through to the surface. This relatively conservative behaviour of $CO_2$ makes it a better proxy of heat release from the shallow reservoir than Cl or measurement of observable heat flow (Chiodini et al., 2005). The main error associated with any $CO_2$ based estimate of reservoir heat release is the selection of a representative molar $H_2O/CO_2$ ratio. The molar ratio of 16.6 is considered representative, though other ratio values produced estimates of 378 or 946MW thermal.

**Spatial and structural relationships of diffuse surface degassing and heat flow**

***Rotokawa***

In general the location of the thermal area at RK is coupled to the location of small prehistoric eruption craters and the major Lake Rotokawa eruption crater. The location of the thermal area at RK coincides with a series of historic hydrothermal explosion craters. The largest of which is the site of Lake Rotokawa. Vigorous surface thermal activity surrounds the explosion craters and includes large outflows of acidic $SO_4$-Cl boiling springs and steaming ground. Most diffuse degassing is coupled to these thermal features and decreases rapidly in magnitude with distance. There are some diffuse degassing areas which show no relationship to Acid $SO_4$-Cl thermal features and even have low temperatures (<50°C) that occur along the lake margins (Figure 3a). Of note there is a major structure along a possible fault escarpment which runs E-W for 300m across the thermal area.

Relationships between diffuse degassing and heat flow at RK are neither purely spatial nor proportional and there are some areas which though cold temperatures are present still produce high gas flux. The locations of these zones near the lake shore indicate a cooling of the soil possibly due to the water table sitting closer to the surface. The present "hot spot" activity at RK indicates multiple areas of high permeability that channel fluid flow.

A high number of these hot spots are located along the northern shore of Lake Rotokawa. Hot spots are typical of permeability being controlled by alteration of clay and the movement of heat and gas through the medium. As an area is flooded with hydrothermal fluid and heat, the local strata will alter to clays over time and at some point a feature which once exploited an area of high primary permeability will seal itself.

The hydrostatic pressure of the lake might act as a barrier which forces the gas to migrate laterally to the lower pressure shoreline and where the gas can rise to the surface, this is evident by bubbling zones within 5m of the shoreline where the water is shallow (<2m) continuing up on to the land.

Historic mining of sulphur has also affected the topography of the thermal area by creating low-lying

surfaces which now intersect with the water table allowing hot springs and steaming ground to formed. In these areas hydrothermally altered clays from the shallow subsurface have been deposited on the surface which reduces permeability.

Deep field faulting can cause hot spots of high permeability that allows boiling fluids to rise. There is a large field fault running through the middle of RK, the Central Field Fault (CFF) of Winick et al. (2011) indirectly influences the diffuse degassing structures with historic eruptions craters that appear to focus thermal activity occurring along its strike. The magnitude of the gas fluxes in the vicinity of these craters and along the strike of the CFF suggests a deep-seated connection between surface eruption craters and the CFF which may be channelling fluids from depth.

***White Island***

The hydrothermal system at WI is actively degassing through permeable areas of the crater floor, crater walls, crater rim, old crater rims and through mound structures on the crater floor (Figure 5a). The mounds host numerous small fumarolic vents that are encrusted with sulphur condensate, are of high temperature and comprised of highly altered clays and are analogous to the diffuse degassing structures (DDS) characterised by Chiodini et al., (2005). The vigour, size and number of DDS along with steaming ground and acidic-Cl outflows increases with proximity to the Crater Lake and the modern day centre of volcanic activity.

Most $CO_2$ is exhausted through the Crater Lake and around its rim there is a high flux zone. In the middle of the crater floor there is an arcuate channel of high flux that aligns closely with an old crater rim. This area is one of the most permeable at WI, with boiling mud pots and steaming ground common. Diffuse degassing, fumaroles, and steaming ground are present at breaks in slope (crater floor/wall, crater wall/rim, crater floor/mound) which are generally places of deposition or erosion, so strata would likely have high permeability.

Elsewhere on the island there are areas of capping clays at around 1m depth that limit degassing locally. These are hypothesised to be the remnants of the old crater floor, consisting of impermeable and altered volcaniclastic material.

**Sulphur Budget (Rotokawa)**

$H_2S$ occurs in background concentrations until $CO_2$ flux becomes advective (Figure 7). Based on interpretations of this phenomenon by Werner et al. (2008) it is assumed that a similar process is occurring at RK, where during low $CO_2$ fluxes, diffusion is the main mechanism and $H_2S$ is removed, but when there is high $CO_2$ flux modest amounts of $H_2S$ reaches the surface.

## CONCLUSION

The hydrothermal systems and their respective surface thermal expressions at RK and WI emit an extraordinary quantity of $CO_2$ and thermal energy per unit area. This study continues with the style and approach of recent soil gas surveys at New Zealand geothermal systems (Rotorua, Werner & Cardellini 2006; Ohaaki, Rissmann et al. 2012) and has found that RK emits the most $CO_2$ per unit area of any measured geothermal field in New Zealand.

This study has produced a steam flux that matches the upflow rate from numerical models based on well gas chemistry.

Areas of high flux are constrained and confirm that deep seated permeability as major normal faults and/or crater rim faults and are paired with surface thermal features. The magnitude of both heat flow and $CO_2$ flux decrease with distance from each feature.

At RK deep field faults appear to have control over the location of thermal activity by controlling the location of hydrothermal eruption craters and subsequent gas release at the surface. At WI the greatest concentration of thermal activity is concentrated above the buried crater rim and along the margins of the modern day crater which suggests a deep-seated channel of fluids along crater rim faults-fracture zones.

A mechanism for $H_2S$ fixing exists in areas of diffuse soil degassing as the concentration of $H_2S$:$CO_2$ in fumarole gas is more than is measured in soil gas.

**Acknowledgements**

Thanks to Mighty River Power Limited (Linda Price, Simon Addison, Jeremy O'Brien, the staff at NAP), Tom Powell, GNS Science (Jeremy Cole-Baker, Karen Britten), University of Canterbury (Jim Cole, Anekant Wandres, Heather Bickerton, Jelte Keeman) and Thrainn Fridriksson. This Study contributes and is funded by the UC-MRP Source 2 Surface joint venture research programme with additional funding from the Foundation for Research, Science, & Technology through a TechNZ Scholarship.

## REFERENCES


Bergfeld, D., Evans, W.C., Howle, J.F., Farrar, C.D., 2006. Carbon dioxide emissions from vegetation-kill zones around the resurgent dome of Long Valley Caldera, eastern California, USA. J. Volcanol. Geotherm. Res. 152, 140–156.

Boomer, K., Werner, C. and Brantley, S.L., (2000): CO2 emissions related to the Yellowstone volcanic system; 1, Developing a stratified adaptive cluster sampling plan. Journal of Geophysical Research, 105(B5): 10817-10830.

Bowyer, D., and Holt, R., 2010, Case Study: Development of a Numerical Model by a Multi-Disciplinary Approach, Rotokawa Geothermal Field. Proc. World Geothermal Congress 2010 Bali, Indonesia, 25-29 April.

Brombach, T., Hunziker, J.C., Chiodini, G., Cardellini, C., Marini, L., 2001. Soil diffuse degassing and thermal energy fluxes from the southern Lakki Plain, Nisyros (Greece). Geophys. Res. Lett. 28, 69–72.

Cardellini, C., Chiodini, G., Frondini, F., 2003. Application of stochastic simulation to $CO_2$ flux from soil; mapping and quantification of gas release. J. Geophys. Res.108 (B9), 13

Chiodini, G., Cioni, R., Guidi, M., Raco, B., Marini, L., 1998. Soil CO 2 flux measurements in volcanic and geothermal areas. Appl. Geochem. 13, 543–552
.
Chiodini, G., Avino, R., Brombach, T., Caliro, S., Cardellini, C., De Vita, S., Frondini, F.,Granirei, D., Marotta, E., Ventura, G., 2004. Fumarolic and diffuse soil degassing west of Mount Epomeo, Ischia, Italy. J. Volcanol. Geotherm. Res. 133, 291–309.

Chiodini, G., Granieri, D., Avino, R., Caliro, S., Costa, A., Werner, C., 2005. Carbon dioxide diffuse degassing and estimation of heat release from volcanic and hydrothermal systems. J. Geophys. Res. 110 (B8), 17.

Collar, R.J. and Browne, P.R.L., 1985, Hydrothermal eruptions at the Rotokawa Geothermal Field, Taupo Volcanic Zone, New Zealand. Proc. 7th NZ Geothermal Workshop. . 1-5.

Dawson, G.B., 1964. The nature and assessment of heat flow from hydrothermal areas. N. Z. J. Geol. Geophys. 7, 155–171

Deutsch, C.V., Journel, A.G., 1998. GSLIB: Geostatistical Software Library and User's Guide. Applied Geostatistics Series. Oxford University Press, New York, Oxford.

Fridriksson, T., Kristjansson, B.R., Armannsson, H., Margretardottir, E., Olafsdottir, S., Chiodini, G., 2006. CO 2 emissions and heat flow through soil, fumaroles, and steam-heated mud pools at the Reykjanes geothermal area, SW Iceland. Appl. Geochem. 21, 1551–1569.

Giammanco, S., Parello, F., Gambardella, B., Schifano, R., Pizzullo, S., Galante, G., 2007. Focused and diffuse effluxes of CO 2 from mud volcanoes and mofette south of Mt. Etna (Italy). J. Volcanol. Geotherm. Res. 165, 46–63.

Giggenbach, W., Matsuo, S., 1991. Evaluation of results from Second and Third IAVCEI field workshops on volcanic gases, Mt. Usu, Japan and White Island, New Zealand. Appl. Geochem. 6, 125–141.

Hedenquist, J.W., Mroczek, E.K., Giggenbach, W.F., 1988, Geochemistry of the Rotokawa Geothermal System: Summary of Data, Interpretation and Appraisal for Energy Development: DSIR Chemistry Division Technical Note 88/6, 64

Hochstein, M.P., Bromley, C.J., 2005. Measurement of heat flux from steaming ground. Geothermics 34, 131–158

Houghton, B.F., Nairn, I.A., 1989. A model for the 1976–82 phreatomagmatic and Strombolian eruption sequence at White Island volcano, New Zealand. In: Houghton, B.F., Nairn, I.A. Ž.Eds. , The 1976–82 Eruption Sequence at White Island Vol-Ž.cano Whakaari , Bay of Plenty, New Zealand. N. Z. Geol. Surv. Bull. 103, pp. 127–137, Rotorua

Mörner, N.-A., Etiope, G., 2002. Carbon degassing from the lithosphere. Global Planet. Change 33, 185–203.

Rissmann, C.F., 2010. Using Surface Methods to Understand the Ohaaki Field, Taupo Volcanic Zone, New Zealand. Unpubl. Doctoral Dissertation. Univ. Canterbury, Christchurch, New Zealand.

Rissmann, C., Nicol, A., Cole, J., Kennedy, B., Fairley, J., Christenson, B., Leybourne, M., Milicich, S., Ring, U., Gravley, D., 2011. Fluid flow associated with silicic lava domes and faults, Ohaaki hydrothermal field, New Zealand. J. Volcanol. Geotherm. Res. 204, 12–26.

Rissman, C., Christenson, B., Werner, C., Leybourne, M., Cole, J., Gravley, D., 2012, Surface heat flow and CO 2 emissions within the Ohaaki hydrothermal field, Taupo Volcanic Zone, New Zealand, Appl. Geochemistry 27, 223-239.

Schmidt, E., Grigull, U., 1979. Properties of Water and Steam in SI-units: 0–800 C, 0–1000 bar. Springer-Verlag, Berlin Heidelberg, R. Oldebourg, München

Sinclair, A.J., (1974): Selection of thresholds in geochemical data using probability graphs. J. Geochem. Explor. 3, 129–149.

Wardell, L.J., Kyle, P.R., Dunbar, N., Christenson, B., 2001. White Island volcano, New Zealand: carbon dioxide and sulfur dioxide emission rates and melt inclusion studies. Chem. Geol. 177, 187–200.

Welles, J.M., Demetriades-Shah, T.H. and McDermitt, D.K., 2001. Considerations for measuring
ground CO2 effluxes with chambers. Chemical Geology, 177(1-2): 3-13.

Werner, C., Cardellini, C., 2006. Comparison of carbon dioxide emissions with fluid upflow, chemistry, and geologic structures at the Rotorua geothermal system, New Zealand. Geothermics 35, 221–238. Werner, C., Brantley, S.L., Boomer, K., 2000. CO 2 emissions related to the Yellowstone volcanic system. 2. Statistical sampling, total degassing, and transport mechanisms. J. Geophys. Res. 105, 10,831–10,846.

Werner, C., Hochstein, M.P., Bromley, C.J., Manville, V.R., Tilyard, D., 2004. CO 2-flux of steaming ground at Karapiti (Wairakei, NZ). Geol. Soc. N. Z. 117A, 115–116

## APPENDIX

### 1: Cumulative Probability Plots

*Individual populations are broken down in terms of mean ($M_i$), proportion ($f_i$) and standard deviation ($\sigma_i$).*

***White Island***

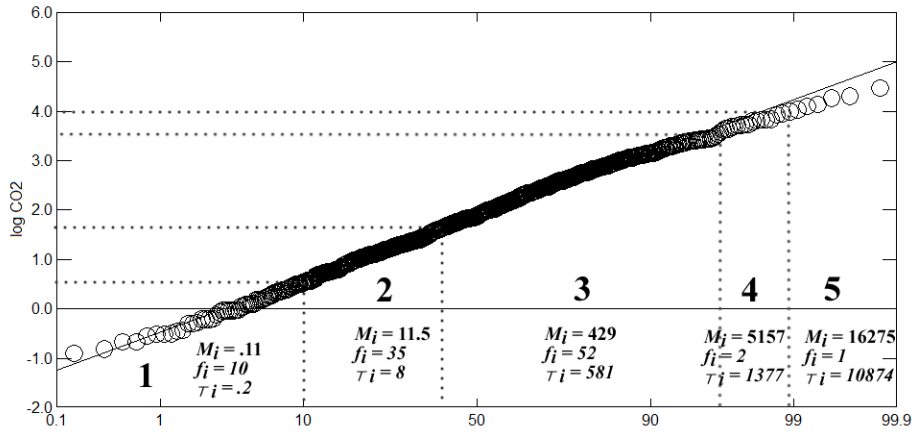


***Rotokawa***

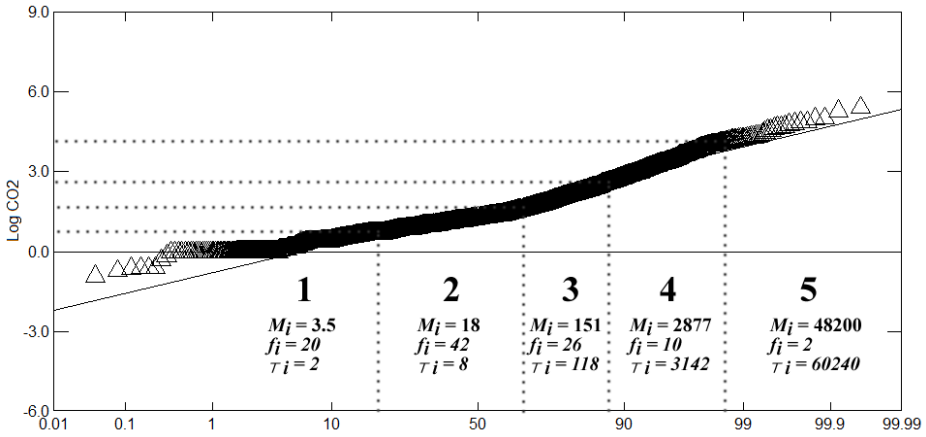


### 2: Variogram Models

Red dotted line is the declustered, normal scores variogram for $CO_2$ Flux.

***Rotokawa***

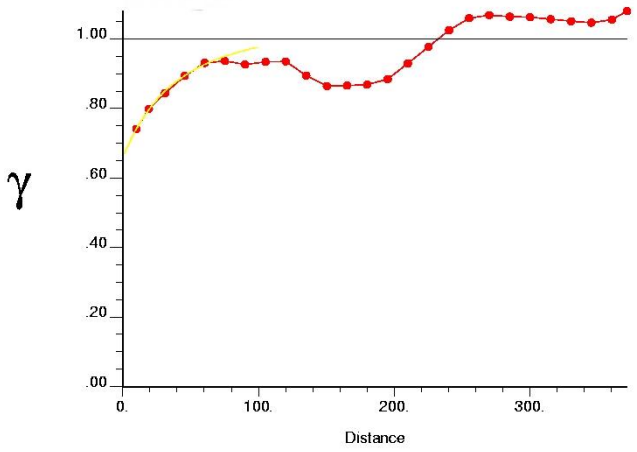


***White Island***